Vol. 05, No. 3 (2023) 439-452, doi: 10.24874/PES05.03.009

Proceedings on Engineering Sciences

www.pesjournal.net

STUDY ON OPEN CONTACT SYSTEMS WITH FLAT PARALLEL ELECTRODES FOR AERIAL ROBOTS CHARGING PLATFORMS

V.S. Fetisov [1]
D.D. Kudashov
A.V. Ovchinnikov
K.O. Novikova

Received 14.12.2022.
Accepted 28.05.2023.
UDC – 007.52

Keywords:

Aerial Robot, Unmanned Aerial Vehicle, Landing, Charging Platform, Open Contact System

A B S T R A C T

The authors of this paper proposed the design of a charging platform for aerial robots (ARs), the advantages of which are the simplicity of implementation, non-requirement of precision landing ARs on the platform and the possibility of servicing several robots simultaneously. The platform comprises a row of flat parallel open electrodes lying in the same plane and separated by thin dielectric spacers. One half of platform electrodes are connected with positive pole of the charging power source and another half – with negative one, and their polarities are interlaced. The AR has several on-board electrodes in its support stanchions, and their contact points are located at the vertices of a regular polygon. Geometric analysis of the on-board electrodes' positions on the platform has been carried out. Practical recommendations have been given for configuring electrodes that can lead to 100% probability of correct contacting. Simulations with the help of the special software were carried out and the probability of correct contacting after landing for different number of contact points under uncertainty of their coordinates was estimated.

1. INTRODUCTION

The term "Aerial Robot" (AR) is used commonly in the field of robotics. It's been known for two decades, and it means a small pilotless flying machine with high degree of intelligence (Michelson, 1998). The better known term is "Unmanned Aerial Vehicle" (UAV) which has long been used in aviation. An AR can be considered as an UAV "capable of sustained flight with no direct human control and able to perform a specific task" (Feron and Johnson, 2008). In other words, ARs is a big class of mobile robots based on UAVs for special tasks that can be performed using their intelligence and autonomy.

There are many types of UAVs based on different flight principles (Liew et al., 2017). This paper deals primarily with the Rotary-Wing type of aerial vehicles (helicopters, multicopters) and other aircrafts (convertiplanes and other hybrids) capable of vertical take-off and landing (VTOL). VTOL UAVs are the closest to common notion of "robots" because of their capability of hovering, which has huge advantages, in comparison with Fixed-Wing aircrafts, for general

[1] Corresponding author: Vladimir Stanislavovich Fetisov
Email: fetisov.vs@ugatu.su

versatility. Perhaps the most popular implementation of AR is the quadcopter due to its successful combination of wealth of opportunities and ease of implementation (Ghazbi et al., 2016).

ARs are designed for various useful functions: aerial photography, monitoring, construction operations, agricultural works, delivery of small packages and so on. One of the most pressing tasks in aerial robotics is on-ground automatic service and maintenance of ARs. This is especially important for the operation of not one single AR, but their groups. Today many well-known companies, as well as new startups specializing in Unmanned Aerial Systems (UAS) (Austin, 2010), are developing various service stations for ARs (Aerobotics, 2022), (H3 Dynamics, 2022), (Noon.21st Century, 2022), (Skycharge, 2022), (WiBotic, 2022).

UAS comprises of one or more UAVs (ARs), along with the technical equipment necessary to operate them and other components (Fetisov, 2021). Full composition of UAS may be different depending on its purposes. UAS provides an infrastructure for working environment of ARs. Important components of UAS are service stations. These are specific objects of UAS infrastructure, mainly intended for refueling or recharging UAVs.

Commonly ARs' power units are fully electrical and on-board power supplies are accumulator batteries of Lithium Ion or Lithium Polymer types. Such batteries provide time duration about 30-40 min for helicopters or multicopters. This time is often not enough to carry out various tasks. The AR therefore must replenish somehow its on-board energy supply after discharging.

Different means are known for recharging on-board batteries of UAVs and thus providing long duration of AR's mission. Among them, for example, is transmission of energy to the flying UAV by laser beam (Cui et al., 2017). There are solutions for replenishing energy of on-board power supplies by means of solar panels (Morton et al., 2015). Many various projects use electromagnetic field based wireless power transfer (Lu et al., 2018), (Nguyen et al., 2020), (Chittoor et al., 2021). But the most effective and the easiest way to implement recharging is periodical landing ARs onto a charging platform with special contact terminals fed by a ground-based DC power source.

A large number of technical solutions based on direct contact between on-board and surface electrodes are known. Many systems use various quick connectors with male plugs and sockets. Some of them have lock devices for reliability of contacting (Lee et al., 2016). One part of such connectors often have funnel-shaped centering housing with inside electrode for easy insertion of a corresponding protruding part with another electrode (Antonini et al., 2019).

Service stations may contain not only charging systems but also special automatic mechanisms for fast battery swapping. Such mechanism removes the discharged battery from the supported AR and replaces it with a freshly charged battery (Toksoz et al., 2011), (Swieringa et al., 2010). In this case, the AR will be held up at the station for the minimum time and the battery removed will be charged after AR's departure. In paper (Kemper et al., 2011) the comparison of simple charging stations with contact terminals of different types and the charging station with swapping of batteries is made. The authors proposed methodology for estimating the economic feasibility of automatic recharging/swapping stations for different applications.

Electrical connection between ground and on-board parts of charging circuit in many cases is worth using platforms with open contact systems (Kemper et al., 2011), (Al-Obaidi et al., 2020), (Fetisov et al., 2014). In this approach commutation of ground and on-board electrodes appears right after landing when AR's undercarriage open electrodes touch and simply lay on ground platform open electrodes (pads, strips). Such solution, unlike the conception of charging stations with fixed plug-in connectors, provides arrangement of charging process even in conditions of inaccurate AR landing. There are no complex operations for connecting and disconnecting plugs after landing and before take-off. And, besides, one platform allows charging for a group of ARs simultaneously.

Typically, open surface electrodes lie in the same plane, but in some projects they are intentionally spaced at different altitudes, as in (Stoyanov, 2014), to facilitate the positioning of the vehicle on the platform and ensure the correct electrical connection between surface and on-board electrodes.

Redundancy of electrodes is used to enable independent positioning of the AR on the platform, with an excess of number of surface or on-board electrodes, or both of them. The number of electrodes exceeding the number of charging source poles, i.e. two, should be considered excess. Typically, the greater the redundancy, the greater the freedom to position the AR. And if there is no redundancy or its degree is small, then various additional positioning devices have to be used to ensure that the docking of the AR on the platform is correct (Galimov et al., 2020).

In this paper the authors present results of studying one type of platforms with open contact pads, namely so-called platforms with flat parallel electrodes (Fetisov and Akhmerov, 2019). Their main advantage is simplicity of implementation, and reliability is quite high if special requirements for geometric parameters of electrodes are met.

This article does not deal with short-range navigation and precision landing of the vehicle on the ground service platform. These tasks are usually performed by on-board and (or) land-based video cameras. Data fusion integrating video information and signals from other sensors (inertial sensors, GPS receiver, barometer) is often used. These issues are relatively well covered in the technical literature (Saripalli et al., 2003), (Conte and Doherty, 2009), (Kendoul et al., 2009), (Kendoul, 2012), (Kong et al., 2013).

This work focuses mainly on the charging platform design and geometric analysis of the mutual positions of the AR's on-board electrodes and electrodes of the platform.

2. CHARGING STATIONS BASED ON LANDING PLATFORMS WITH FLAT PARALLEL ELECTRODES

The general idea of the proposed charging station (Fetisov et al., 2013) (Figure 1) uses redundancy of platform electrodes. It consists of a row of flat parallel electrodes implemented as metal stripes lying in the same plane and separated from each other by narrow insulating spacers. One half of platform electrodes are connected with positive pole of the charging power source and another half – with negative one, and their polarities are interlaced. Let's the AR has 4 on-board landing electrodes positioned at the end of the AR's legs. Due to special geometrical features of the platform and on-board electrodes different polarities of the on-board electrodes would be obtained under any position of the AR on the station. That is at least one on-board electrode would be of different polarity than others (condition of heteropolarity). The special on-board distributing diode circuit provides right connection of the on-board battery charging controller to the platform power source under any random combination of on-board electrodes' polarities (Figure 1, a). The charging controller is connected to the accumulator battery GB1.

If the width of the platform electrode is a, the width of the insulating spacer is δ, and the length of the side of a square which vertices correspond to the contact points of on-board electrodes is d, then the geometrical condition providing 100% probability of heteropolarity of on-board electrodes is the equality $d=a+\delta$. Due to the small size of δ we shall count $d=a$ (Figure 1, b).

Circuits of balancing battery cells and circuits of disconnection of on-board electronics during charging time are not shown in figure 1, a. Due to the special form of insulating spacers and ends of on-board landing electrodes short circuit between neighboring platform electrodes via a landing electrode is practically impossible.

The described charging station may be used for service of a few ARs simultaneously (Figure 2).

3. DESIGN OF ELECTRODES

For right positioning on-board electrodes on the ground platform and excluding situations when the on-board electrode lays on two adjacent platform electrodes simultaneously or gets stuck on the insulator's edge ends of on-board electrodes must be rather sharp (Figure 1, b). The contact area therefore is small. This fact makes it necessary to limit charging current and leads us to find a solution to improve reliability of contacting.

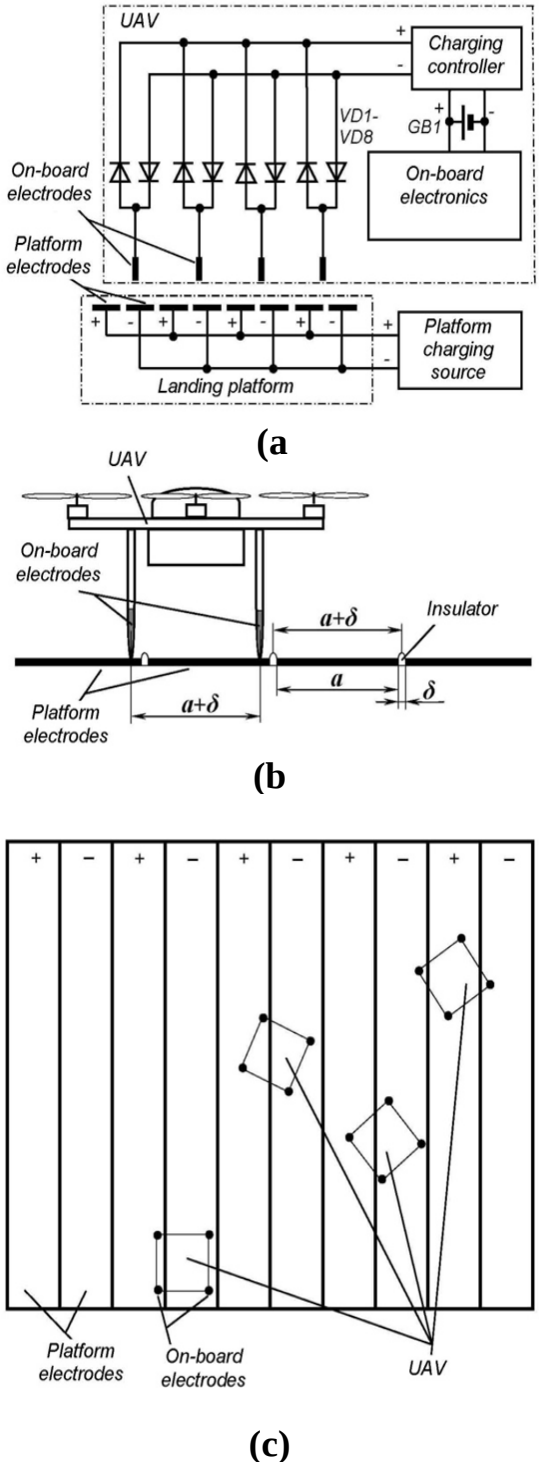

Figure.1. Charging station with flat parallel electrodes: a – station structure; b – UAV positioning on the platform flat electrodes; c – random locations of on-board electrode contact points on the landing platform.

Improved contacting can be achieved in a number of ways:

- use of protective metal coatings,
- increasing the number of on-board electrodes,
- increasing the force of pressing on-board and ground electrodes together by the use of magnetic or electromagnetic elements (Mulgaonkar, 2012),
- providing conditions for all on-board electrodes to be pressed uniformly and qualitatively against strips of the platform.

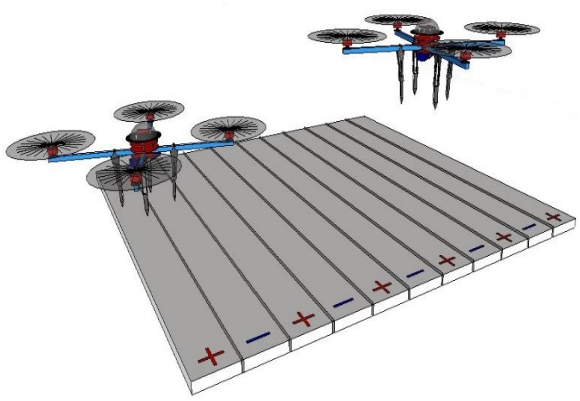

Figure 2. A charging station based on a platform with flat parallel electrodes can serve multiple ARs simultaneously.

The latter can easily be achieved by spring-loading on-board electrodes. But it's not the only option. For example, figure 3 illustrates the technical solution in which an increase in the contact area is achieved by landing the AR on strips in the form of soft metal mats.

It is obvious that in case of landing on a soft strip its deformation thereof will contribute to "wrapping" the lower part of the tip with the deformed surface of the strip and to multiplying the contact area of the electrodes.

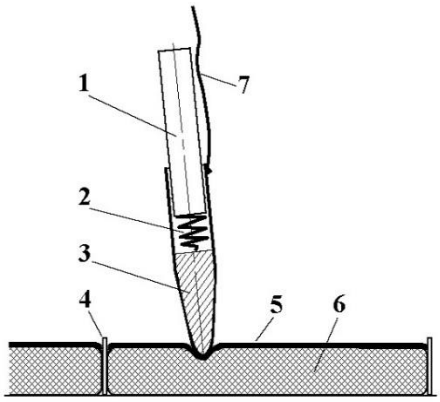

Figure 3. The technical solution with spring-loaded electrodes and soft on-ground strips: 1 – rod of UAV landing gear (support stanchion), 2 – metal spring, 3 – metal tip (on-board landing electrode), 4 – dielectric separator, 5 – metallized coating, 6 – soft elastic material, 7 – current-carrying wire.

4. GEOMETRIC ANALYSIS OF ON-BOARD ELECTRODES POSSIBLE POSITIONS

In the above example (Figure 1), a UAV has four on-board landing electrodes. This case is typical of quadcopters, where it is convenient to place electrodes-stanchions under the motor-bearing beams of the device frame. In other cases, the number of on-board landing electrodes may also be chosen according to the number of bearing beams. For example, it is better to have three on-board landing electrodes for tricopter and six for hexacopter. And it is naturally to place contact points of them in the vertices of regular polygons. Further we will examine in more detail some of the options for the location of the contact points. Only those variants of location are considered acceptable for which the probability of the ends of all electrodes falling onto strips of only one polarity is zero. That is, the situation of unipolarity for all contact points should be excluded.

4.1. Location of contact points at the vertices of a triangle

Of all geometric variants for triangles, only the position of the contact points on the vertices of a regular (equilateral) triangle is permissible. Figure 4 shows two near-critical but tolerable positions of contact points for this case. Still consider δ negligible in comparison to a.

For the first variant shown in figure 4 (length of side $c_1 = a$), it is clear that, if the triangle is rotated, it is possible to make such a landing when all three touching points are on the same strip. For the second variant (the width of the strip a equals the height of the triangle: $h = c_2 \cos 30^\circ$) such situation is excluded. At any rotations, one point of contact will lie on the adjacent strip relative to the other two. Therefore, it is better to select

$$c_2 = a/\cos 30^\circ \approx 1.155 \cdot a.$$

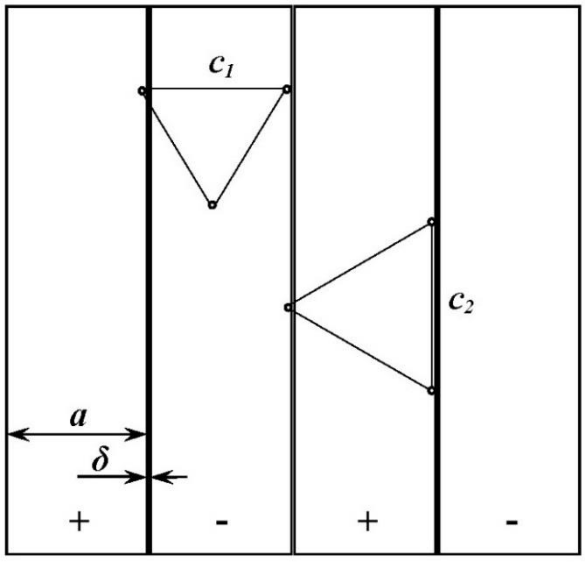

Figure 4. Near critical positions of the contact points at the vertices of regular triangles.

A further lengthening of the side of the triangle is not permissible, as it is possible for two vertices on the base of the triangle to be on the same strip and for the opposite vertex to be on the strip «through one» (i.e. the polarity of all three vertices will be the same). For these reasons, touching points cannot be placed at the vertices of an unequal triangle.

Positioning the contact points of on-board electrodes at the vertices of the triangle has one clear advantage over all other possible variants (such as vertices of square, hexagon, octagon and so on): uniform pressurization of all on-board electrodes to the planes of the ground electrodes is guaranteed at all times, even if there are different irregularities, distortions and differences in the planes of the ground electrodes. For multicopters with four or more on-board electrodes, all electrodes have to be pressed uniformly by special measures (Figure 3).

4.2. Location of contact points at the vertices of a square

This option has already been considered above. To meet the heteropolarity condition of on-board electrodes, it is necessary to maintain equality $d=a$, where d is the distance between adjacent contact points (the length of the side of a square). Positioning the contact points at the vertices of a rectangle is not acceptable, as all four of the on-board electrodes may be on strips with the same polarity.

Four landing electrodes can be found not only in quadcopters, but also in vehicles with higher number of rotors. For example, figure 5 shows hexacopter and octocopter whose support stanchions are not made under each motor-bearing beam. At the ends of these stanchions, electrodes can be formed whose contact points fall into the vertices of the square.

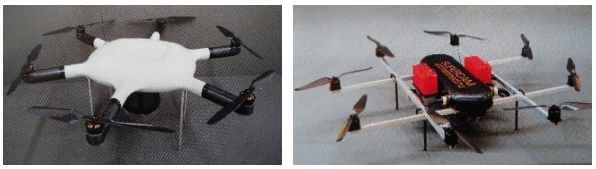

Figure 5. Hexacopter and octocopter with four support stanchions.

However, increasing the number of on-board electrodes can provide high charging currents. And from this point of view, the configuration of the on-board electrode system in which they are located under each beam of a multicopter at the vertices of regular polygons has some advantage. In addition, as will be shown below, configurations with high number of on-board electrodes provide a higher probability of successful landing that ensures the heteropolarity of on-board electrodes.

Then next consider the location of the contact points at the vertices of a regular hexagon (configuration for a hexacopter).

4.3. Location of contact points at the vertices of a regular hexagon

Similar to figure 4, figure 6 shows two near-critical but tolerable positions of contact points for this case. It is not difficult to see that the length of the side of the hexagon must be at least g_1 (to prevent all vertices from falling into the same strip) and at most g_2 (to prevent the opposite triads of the vertices from being through a strip from each other).

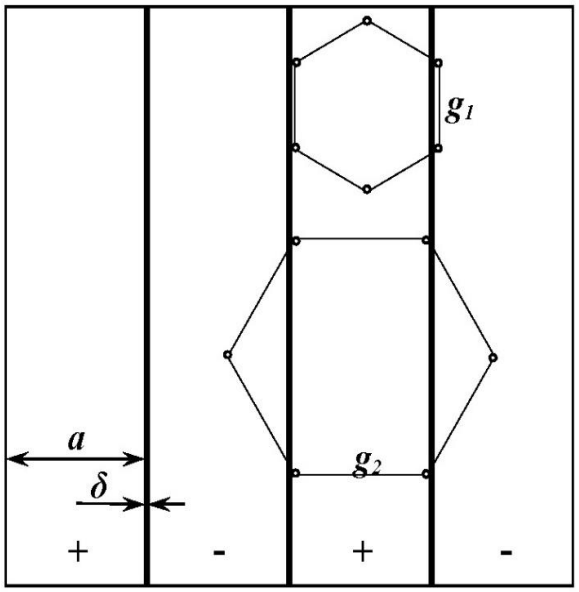

Figure 6. Near critical positions of the contact points at the vertices of regular hexagons.

Simple geometric calculations yielded the following inequalities for the side of the hexagon g:

$$a/(2\cos 30^\circ) = 0.577a < g < a.$$

4.4. Location of contact points at the vertices of a regular octagon

As in the previous case, consider two critical lengths of the polygon side (f_1 and f_2 shown in Figure 7). This length of the side of the octagon must be at least f_1 (to prevent all vertices from falling into the same strip) and at most f_2 (to prevent the opposite tetrads of the vertices from being through a strip from each other).

From simple geometric calculations we get the next double inequality for the side of the octagon f:

$$a\cdot\tan 22.5^\circ = 0.414a < f < a.$$

4.5. Geometric analysis summary results

The results of the geometrical analysis that has been performed in 3.1–3.4 we placed in the summarizing table (Table 1). The optimal side lengths for regular polygons (c, d, g, f for triangles, squares, hexagons and octagons respectively) with contact points at their vertices are expressed by the strip width a. In addition, similar expressions are given for the circumcircle radius R for each polygon. This parameter is suitable for the simulation program described below. There is a known

formula linking R to the length x of the side of a generalized regular polygon: $R=x/(2\sin(180°/n))$, where n is the number of sides of a regular polygon.

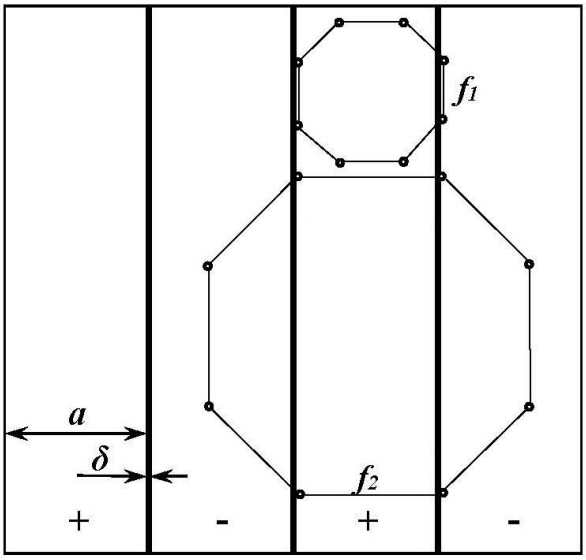

Figure 7. Near critical positions of the contact points at the vertices of regular octagons.

Column 4 of Table 1 contains expected optimums of the polygon side length and the circumcircle radius R at the fixed value of the strip width a = 200 mm. This value will also be used later in simulations.

Table 1. Theoretically calculated optimal ratios* between the geometry of the electrodes and the strip width a

Number of on-board electrodes (Number of regular polygon sides)	Regular polygon side length symbol	The optimal length of the polygon side and the circumcircle radius R expressed by the strip width a	Expected optimums of polygon side lengths, mm and the circumcircle radius R, mm at a = 200 mm
1	*2*	*3*	*4*
3	*c*	$c = 1.155a$ $R = 0.667a$	$c = 231$ $R = 133.4$
4	*d*	$d = a$ $R = 0.707a$	$d = 200$ $R = 141.4$
6	*g*	$0.577a < g < a$ $0.577a < R < a$	$115.4 < g < 200$ $115.4 < R < 200$
8	*f*	$0.414a < f < a$ $0.541a < R < 1.307a$	$82.8 < f < 200$ $108.2 < R < 261.4$

* Optimal geometrical conditions correspond to 100% probability of heteropolarity of on-board electrodes.

5. SIMULATION SOFTWARE

It is of practical interest how the probability of correct electrical connection of the on-board and ground parts of the charging system depends on the number of contact points, the size length of the corresponding regular polygon, and the uncertainty of the contact points' positions.

Estimating the probability of the correct position of the apparatus on the platform in an analytical form is rather problematic, so such estimation was made using the special software simulator, called CoptersLanding. The program allows to simulate random positions of the air robot on the platform, to analyze the polarity of contact points of the on-board electrodes and to calculate the percentage of successful and unsuccessful landings.

In Options Area of the program (Figure 8, on the right), the user can set the number of strips, length and width of strips, the number of on-board electrodes (contact points), the circumcircle radius for the regular polygon whose vertices coincide with contact points, and the uncertainty of the coordinates of the contact points (maximum random deviation of coordinates from given values). The user can set the single run or multiple runs of simulation.

The Results Area window of the program displays the result of the simulation (Figure 9, on the left). For all runs of simulation the polarity of each contact point is shown and the result of the landing - successful (I) or unsuccessful (O, in case of the same polarity for all contact points).

The final result is represented by the number of simulation runs and the percentage of correct landings (Figure 9, the upper-left corner), which, if the number of runs is large enough, can be considered with some degree of approximation as a probability of successful landing.

The central part of the software window shows the view of the landing platform with strips of electrodes and images of all random landings represented as positions of contact points.

Only those landings for which all contact points of the UAV are placed on the platform without crossing its borders are evaluated.

The program allows to emulate simultaneously the AR random position on the platform and random deviations of coordinates of all contact points.

With a large number of statistical tests (in all simulations it was given at 10000), it is possible to get a reasonably reliable estimate of the probability of successful landings).

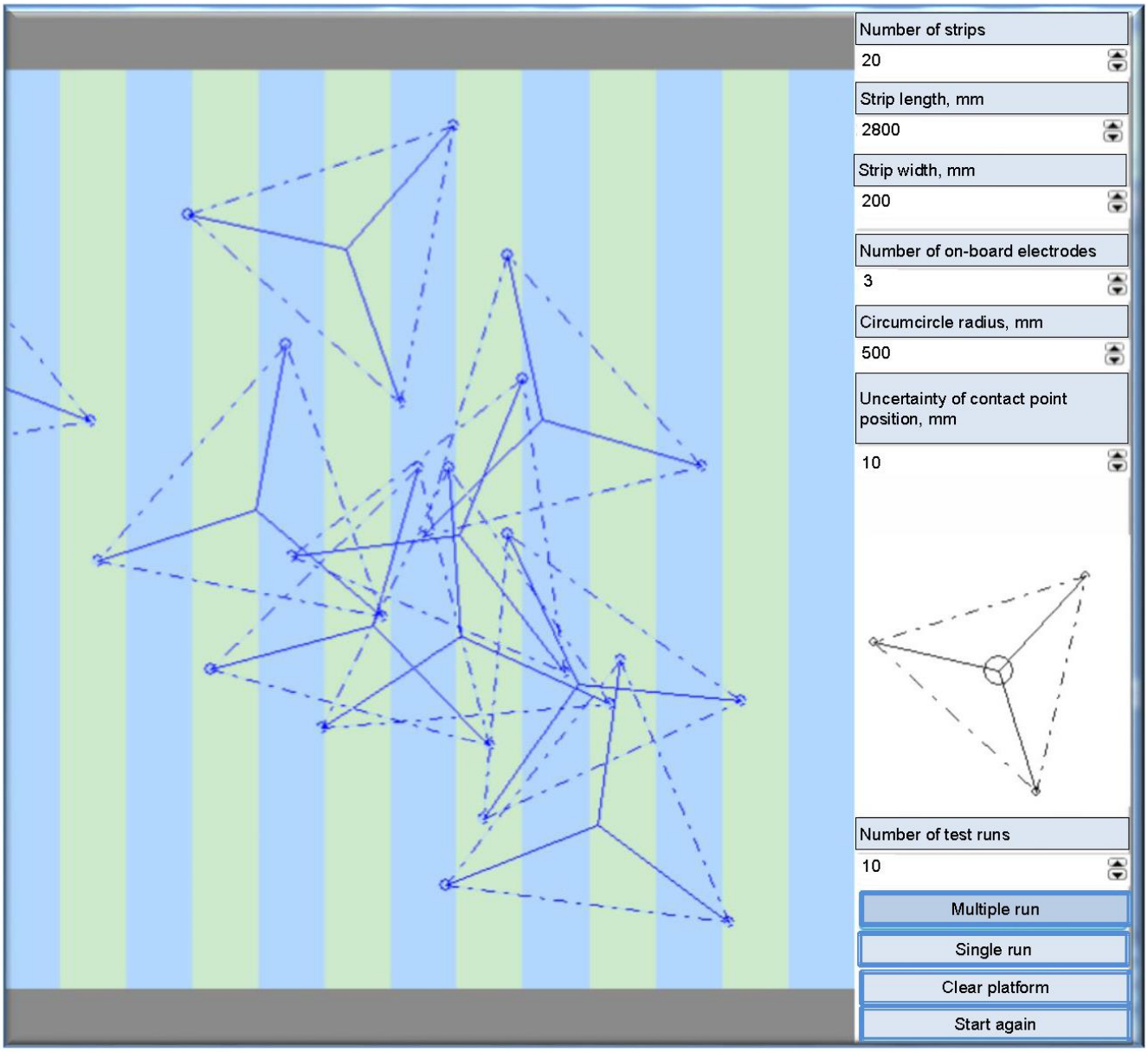

Figure 8. CoptersLanding Options Area (on the right).

In all the evaluated cases of landings, the following geometrical parameters of the platform were given constant:

- number of strips: 20;
- strip length: 3000 mm;
- strip width: 200 mm.

The following parameters were varied:

- number of on-board electrodes: 3, 4, 6, 8;
- radius of the circumcircle: 50–400 mm;
- uncertainty of the contact points coordinates (limit values of random deviations with uniform probability distribution law): 0, 3, 5, 7, 10 mm.

6. SIMULATION RESULTS

Random landing simulation results for the case of the absolutely exact location of contact points at the vertices of regular polygons (the uncertainty of coordinates of contact points γ=0) are represented in the graphs of Figure 10.

The theoretical predictions shown in Table 1 have been fully confirmed by simulation results.

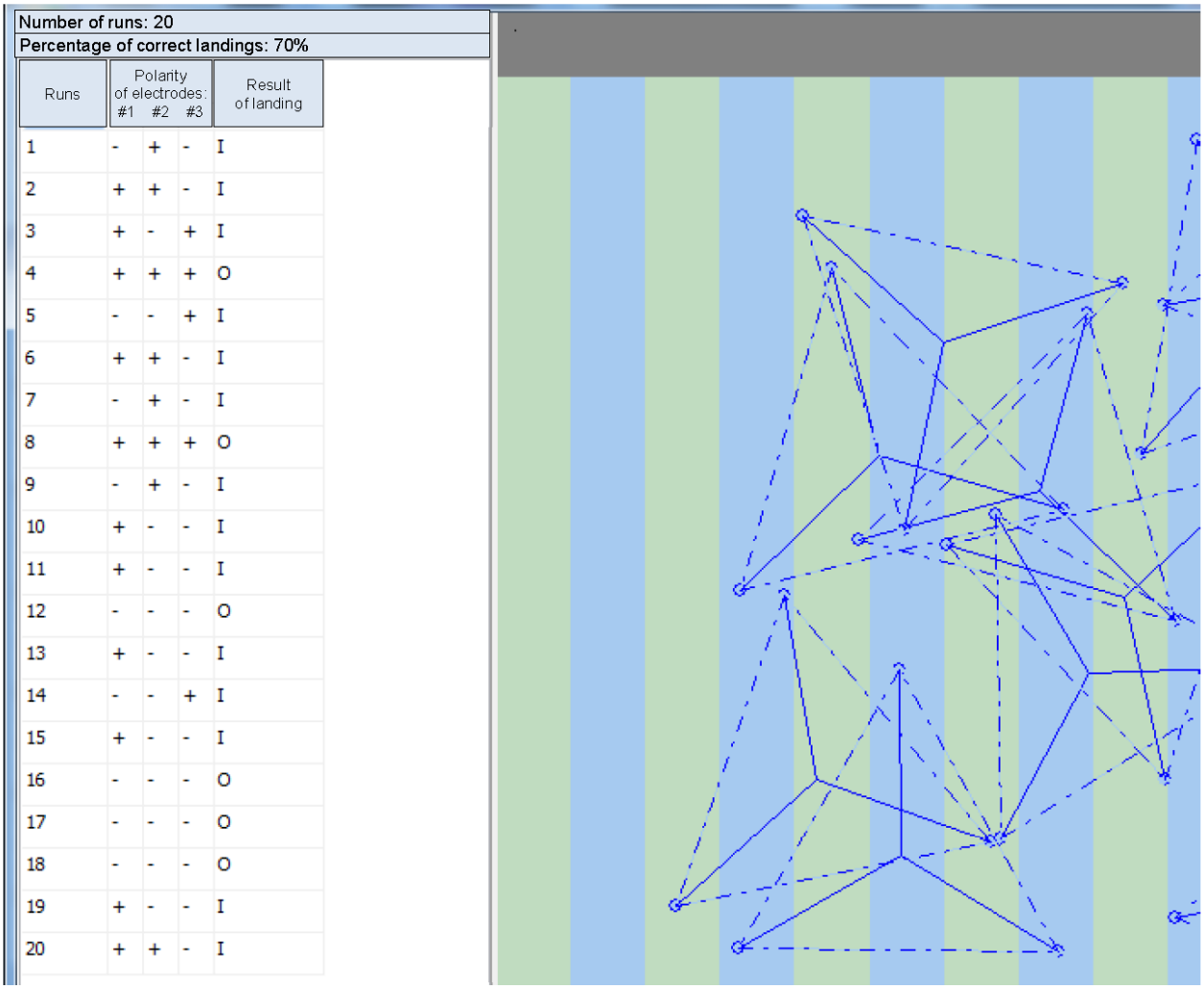

Number of runs: 20
Percentage of correct landings: 70%

Runs	Polarity of electrodes: #1	#2	#3	Result of landing
1	-	+	-	I
2	+	+	-	I
3	+	-	+	I
4	+	+	+	O
5	-	-	+	I
6	+	+	-	I
7	-	+	-	I
8	+	+	+	O
9	-	+	-	I
10	+	-	-	I
11	+	-	-	I
12	-	-	-	O
13	+	-	-	I
14	-	-	+	I
15	+	-	-	I
16	-	-	-	O
17	-	-	-	O
18	-	-	-	O
19	+	-	-	I
20	+	+	-	I

Figure 9. CoptersLanding Results Area (on the left).

For all tested variants of the contact points' location (3, 4, 6, 8 points) there are optimal ranges of the AR's geometric parameters (radius of the circumcircle R), at which the landing will always be successful in the sense of the correct commutation of electrodes. Furthermore, as can be seen from Figure 10(a – c), the optimality zone expands as the number of contact points increases.

Somewhat unexpected was the presence of a zone of minimal probability of successful landing following the maximum zone (it is visible, with varying degrees, on each of the graphs of Figure10(a – c). Then again, the probability increases, though not always to 100%.

It would be difficult to predict theoretically the behaviour of the curve in this area. Therefore, a simulated computational experiment to assess the probability of a successful landing is practically the only reliable means.

A special series of simulations was implemented to estimate how the uncertainty of the contact points' coordinates γ affects the probability of successful landing

p. Limit values of 0, 3, 5, 7, 10 mm were given successively for γ. These are typical values for real conditions, when the uncertainty of coordinates may be due to factors such as technological errors in the installation of the on-board electrodes or the inflexibility of the supports. The ranges of R within and in close proximity to the above-mentioned optimum zones were the most interesting to study. The behavior of the dependencies $p = f(R)$ for the values γ = 0, 3, 5, 7, 10 mm was studied in detail. The results for 3-, 4- and 6-point contact schemes are presented in Figure 11-13.

The graphs show that for 3- and 4-point contact schemes where the optimal zone of R is relatively narrow, it is almost impossible to achieve a 100% successful landing at γ =5 mm and more.

For 6- and 8-point schemes (the graphs for 8-point scheme are not shown here, because they are similar to the graphs for 6-point scheme shown), starting with

certain R values (in Figure13, the values of $R \approx 126$ mm), the uncertainty γ ceases to have any effect on the probability of successful landing.

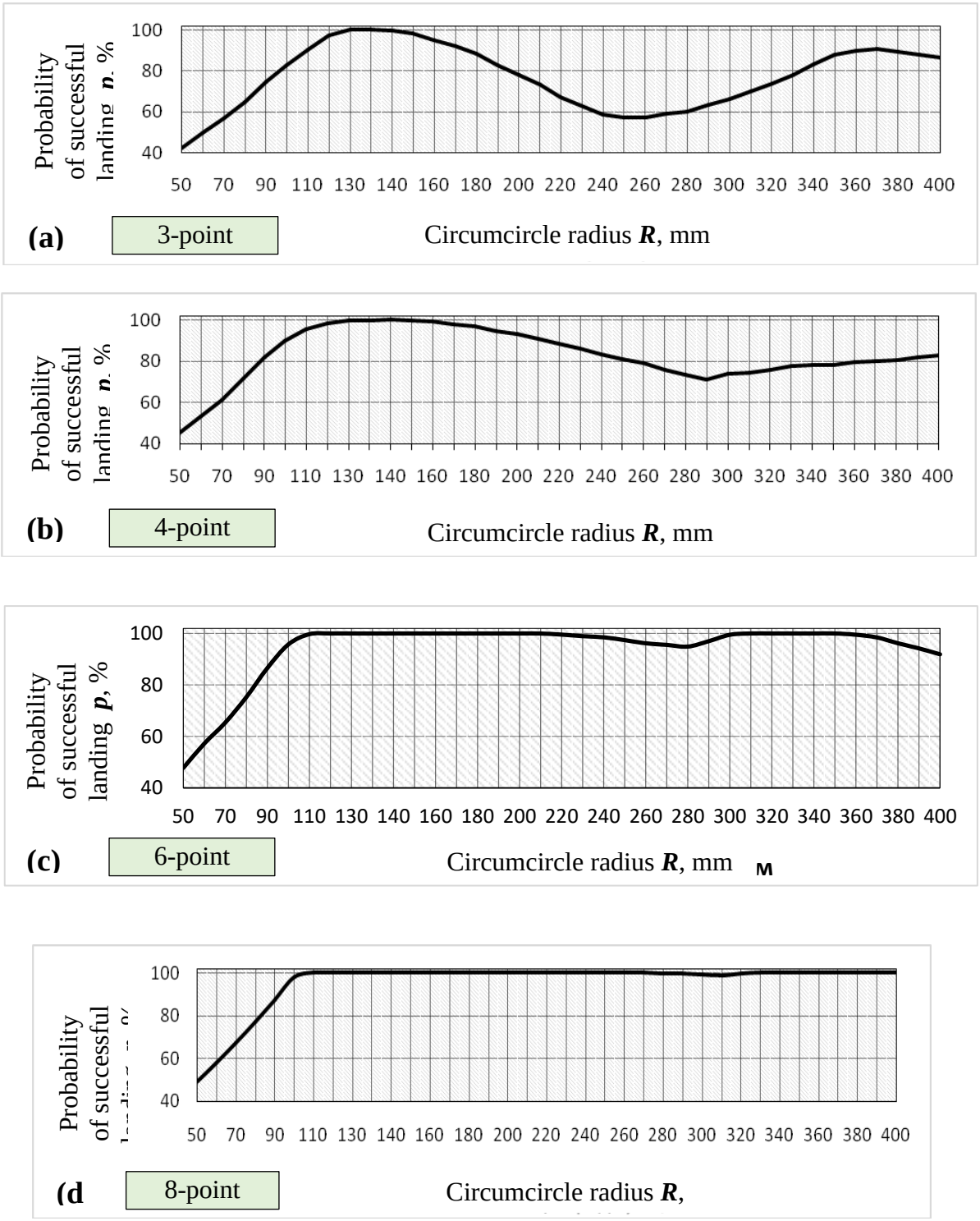

Figure 10. Probability of successful landing vs. circumcircle radius for different contact schemes: (a) 3-point scheme, (b) 4-point scheme, (c) 6-point scheme and (d) 8-point scheme.

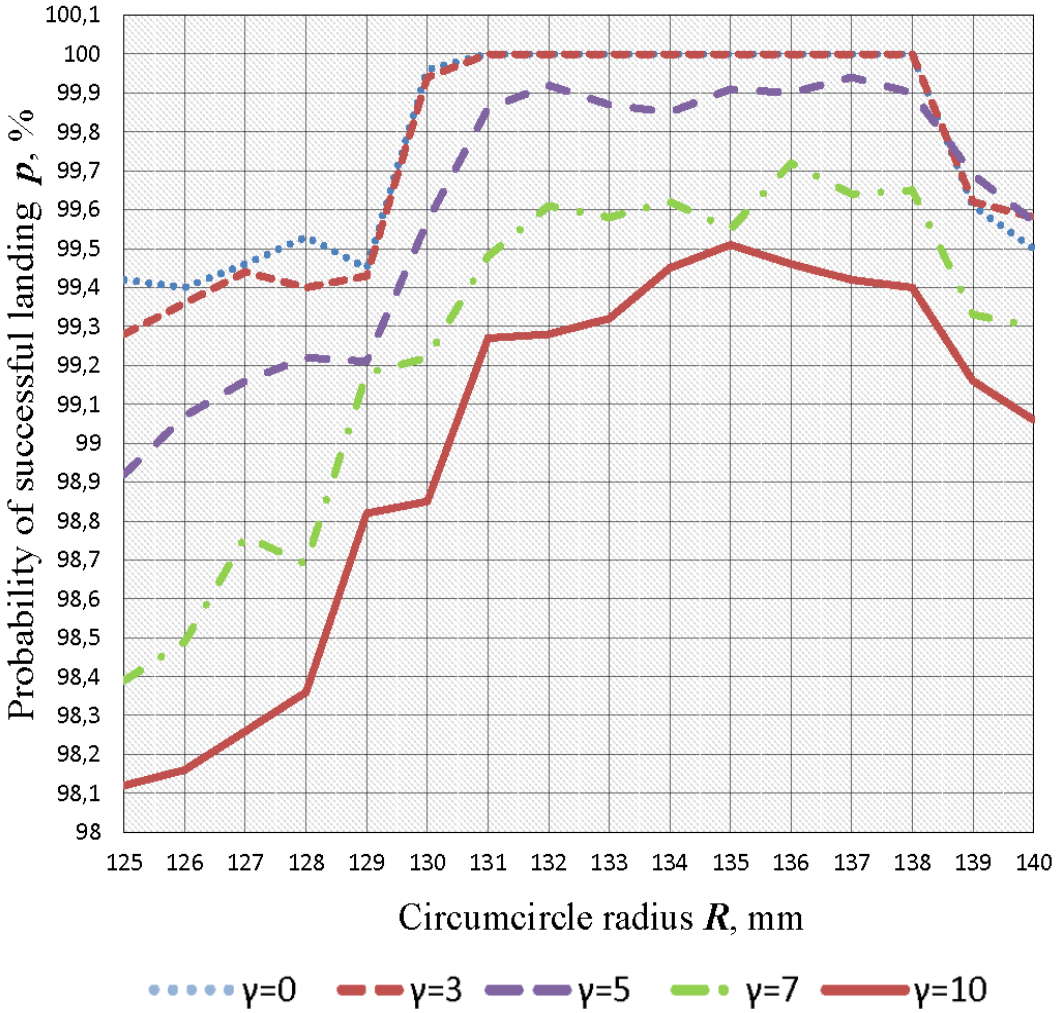

Figure 11. Probability of successful landing vs. circumcircle radius for 3-point contact scheme at different uncertainties of contact points' coordinates γ.

The range of values of R where p =100% at any values of γ < 10 mm continues to the right up to values about 260 mm for the 6-point contact scheme, and never ends at all for the 8-point contact scheme.

7. CONCLUSION

The developed simulation program made it possible to estimate the probability of successful landing of an aerial robot having regular arrangement of on-board electrodes (their contact points are located at the vertices of a regular polygon) on the charging platform that has flat parallel electrodes of interlaced polarity. Landing is considered successful if the condition of heteropolarity for on-board electrodes is met, i.e. when in contact with strips, at least one on-board electrode shall have a polarity different from others.

The proposed methodology and tool can help to choose the right relationship between the geometrical parameters of the landing platform and the aerial robot.

In order to maximize the probability of a correct landing, it is necessary to observe the special geometric relationship between the width of the ground electrode a and the distance between contact points of adjacent on-board electrodes (side length of a regular polygon), namely, according to Table 1:

- for 3-point contact scheme the distance between adjacent contact points must be 1.155a;
- for 4-point contact scheme the distance must be a;
- for 6-point contact scheme the distance must be between 0.577a and a;
- for 8-point contact scheme the distance must be between 0.414a and a.

Increasing the number of contact points extends the range of tolerable distances between adjacent of them when the probability of a correct landing is 100 %.

The latter conclusion is particularly important for conditions where contact points' coordinates are unstable. If, for example, random deviations of the

contact points' coordinates are 5-10% of circumcircle radius *R*, it is impossible to reach 100% chance of a successful landing for 3-point and 4-point contact schemes (Figures 11, 12), but this is possible for 6-point and 8-point schemes, and the range of tolerable distances between adjacent contact points is rather wide.

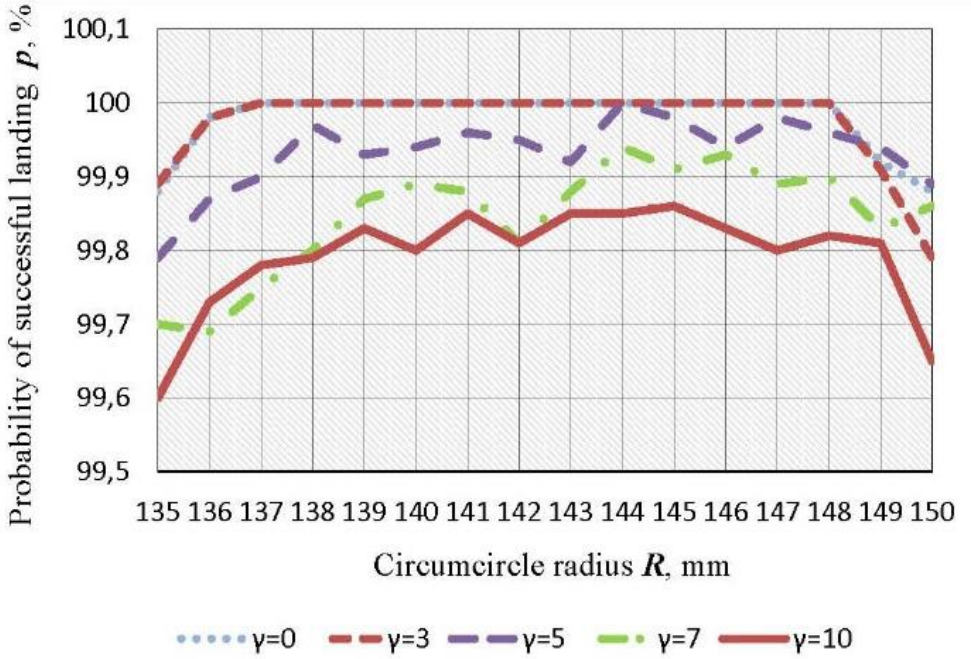

Figure 12. Probability of successful landing vs. circumcircle radius for 4-point contact scheme at different uncertainties
of contact points' coordinates γ.

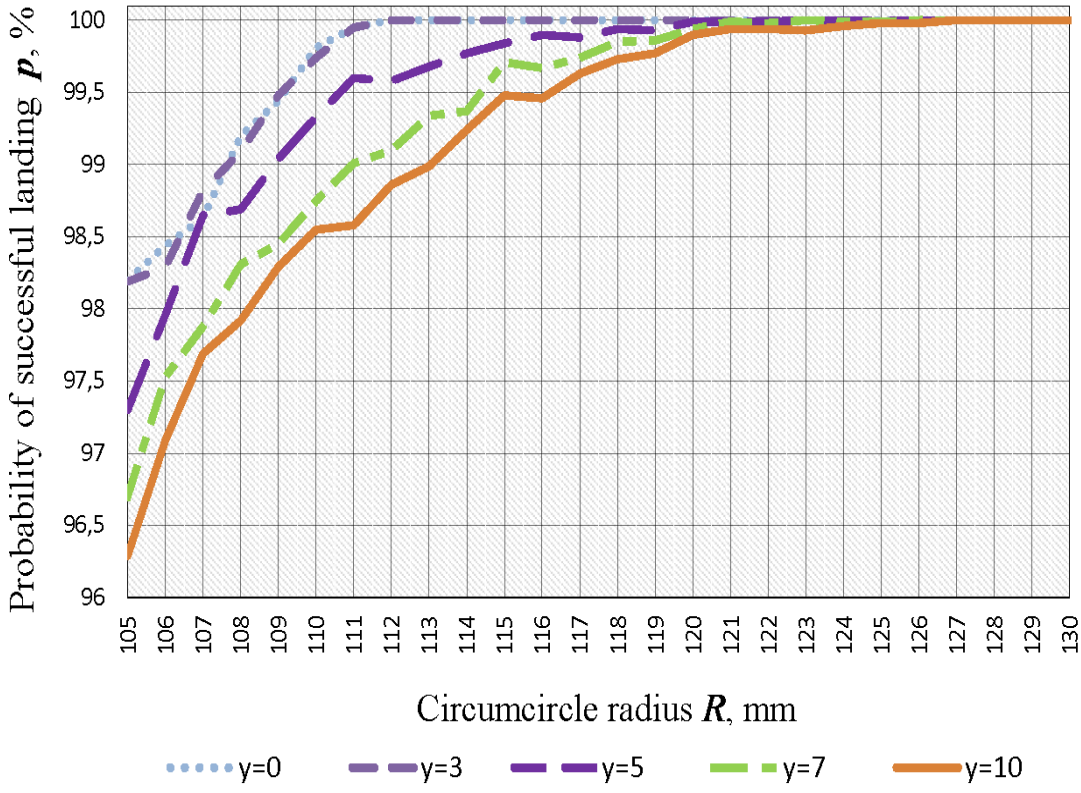

Figure 13. Probability of successful landing vs. circumcircle radius for 6-point contact scheme at different uncertainties
of contact points' coordinates γ.

References:

Aerobotics (2022). Official website. *Automated drones*. Retrieved from https://www.airoboticsdrones.com.

Al-Obaidi, M. R., Mustafa, M. A., Hassan, W. Z. W., Azis, N., Sabry, A. H., & Ab-Kadir, M. Z. A. (2020) Improvement in energy conversion for unmanned aerial vehicle charging pad, *Indonesian Journal of Electrical Engineering and Computer Science*, *17*(2), 767-773. doi:10.11591/IJEECS.V17.I2.PP767-773.

Antonini, R., Fici, G. P., & Gaspardone, M. (2019) Landing platform for an unmanned aerial vehicle, *US Patent* № 10434885 B2.

Austin, R. (2010) *Unmanned Aircraft Systems – UAVs Design, Development and Deployment*.

Chittoor, P. K., Chokkalingam, B., & Mihet-Popa, L. (2021) A review on UAV wireless charging: fundamentals, applications, charging techniques and standards, IEEE Access 9, 69235-69266. doi:10.1109/ ACCESS.2021.3077041.

Conte, G., & Doherty, P. (2009) Vision-based unmanned aerial vehicle navigation using geo-referenced information, *EURASIP Journal on Advances in Signal Processing*. doi:10.1155/2009/387308.

Cui, Z. H., Hua, W. S., Liu, X.G., Guo, T., &Yan, Y. (2017) Key technologies of laser power transmission for in-flight UAVs recharging, *IOP Conference Series Earth and Environmental Science*, *61*(1). doi:10.1088/1755-1315/61/1/012134.

Feron, E., &Johnson, E. N. (2008). Aerial Robotics, in *Springer Handbook of Robotics*, 1009-1029.

Fetisov, V. S. (2021) Aerial robots and infrastructure of their working environment, In *Proceedings of 15th International Conference on Electromechanics and Robotics "Zavalishin's Readings*, Springer, Singapore, 3-23.

Fetisov, V., & Akhmerov, S. (2019) Charging stations with open contact pads for maintenance of aerial robots, *International Conference on Electrotechnical Complexes and Systems (ICOECS*). doi:10.1109/ICOECS46375.2019.8949996.

Fetisov, V. et al. (2013) Charging system for aerial robot onboard accumulator, *RU utility model patent* № 135469.

Fetisov, V. S. et al. (2014) Charging system for electrical UAV's battery, *RU Patent* № 2523420.

Galimov, M., Fedorenko, R., & Klimchik, A. (2020) UAV positioning mechanisms in landing stations: classification and engineering design review, *Sensors, 20* (13), 3648. doi:10.3390/s20133648.

Ghazbi, S. N., Aghli, Y., Alimohammadi, M. &Akbari, A. A. (2016) Quadrotors unmanned aerial vehicles: a review, *International Journal on Smart Sensing and Intelligent Systems*, *9*(1), 309-333. https://doi.org/10.21307/ijssis-2017-872.

H3 Dynamics (2022). Official website. *Autonomous Drone Stations as a Service*. Retrieved from https://www.h3dynamics.com/drone-in-a-box-autonomous-aerial-operations-and-services.

Kemper, P., Suzuki, K., &Morrison, J. (2011) UAV consumable replenishment: design concepts for automated service stations, *Intelligent & Robotic Systems 61*(1), 369-397. doi:10.1007/s10846-010-9502-z.

Kendoul, F. (2012) Survey of advances in guidance, navigation, and control of unmanned rotorcraft systems, *Journal of Field Robotics*, *29*(2), 315–378. DOI:10.1002/rob.20414.

Kendoul, F., Nonami, K., Fantoni, I., & Lozano, R. (2009) An adaptive vision-based autopilot for mini flying machines guidance, navigation and control, *Autonomous Robots 27*(3), 165–188. doi:10.1109/IROS.2013.6696776.

Lee, S.C. et al. (2016) Post-type apparatus for containing and charging unmanned VTOL aircraft and method of containing and charging unmanned VTOL aircraft using the same, *US Patent* № 2016/0347192 A1.

Liew, C.F., DeLatte, D., Takeishi, N., &Yairi, T. (2017) *Recent developments in aerial robotics: a survey and prototypes overview*. Online publication. https://doi.org/10.48550/arXiv.1711.10085.

Lu, M., Bagheri, M., James, A. P., & Phung, T. (2018) Wireless charging techniques for UAVs: a review, reconceptualization, and extension, *IEEE Access*, *6*, 29865-29884, doi:10.1109/ACCESS.2018.2841376

Michelson, R. C. (1998) International aerial robotics competition - The world's smallest intelligent flying machines, in Proc. *13th RPVs/UAVs International Conference*, 31.1–31.9.

Morton, S., D'Sa, R., & Papanikolopoulos, N. (2015) Solar powered UAV: design and experiments, in Proc. *IEEE/RSJ International Conference on Intelligent Robots and Systems*, 2460-2466. DOI:10.1109/IROS.2015.7353711.

Mulgaonkar, Y. (2012) *Automated recharging for persistence missions with multiple micro aerial vehicles*, (Master's thesis), Dept. of Mechanical Engineering and Applied Mechanics, University of Pennsylvania.

Nguyen, M. T., Nguyen, C. V., Truong, L. H., Le, A. M., Quyen, T. V., Masaracchia, A., &Teague, K. A. (2020) Electromagnetic field based WPT technologies for UAVs: a comprehensive survey, *Electronics*, *9*(3), 461. DOI:10.3390/electronics9030461.

Noon.21st Century (2022). Official website. *UAV Docking Station*. Retrieved from https://1221.su/uav-docking-station.

Saripalli, S., Montgomery, J., &Sukhatme, G. (2003) Visually guided landing of an unmanned aerial vehicle, *IEEE Transactions on Robotics and Automation, 19*(3), 371-381. doi:10.1109/TRA.2003.810239.

Skycharge (2022). Official website. *Automatic drone/robot-charging requiring no human interaction*. Retrieved from https://www.skycharge.de.

Stoyanov, Yu. P. (2014) Method for charging accumulator batteries of unmanned aerial vehicles, *RU Patent* № 2593207.

Swieringa, K. A., Hanson, C. B., Richardson, J. R., White, J. D., Hasan, Z., Qian, E., &Girard, A. (2010) Autonomous battery swapping system for small-scale helicopters, *2010 IEEE International Conference on Robotics and Automation*, 3335–3340. doi:10.1109/ROBOT.2010.5509165

Toksoz, T., Reddingy, J., Michini, M., Michini, B., How, J., Vavrina, M., & Vian, J. (2011) Automated battery swap and recharge to enable persistent UAV missions, in *Proceedings of AIAA Infotech@Aerospace Conference*. DOI:10.2514/6.2011-1405.

WiBotic (2022). Official website. *Aerial Applications*. Retrieved from https://www.wibotic.com/applications/aerial.

Vladimir Stanislavovich Fetisov
Ufa State Aviation Technical University (USATU),
Ufa,
Russia
fetisov.vs@ugatu.su
ORCID 0000-0002-2065-5077

Alexey Vladimirovich Ovchinnikov
Ufa State Aviation Technical University (USATU),
Ufa,
Russia
ovchinnikov.av@ugatu.su
ORCID 0000-0003-1313-9397

Dmitry Dmitriyevich Kudashov
Ufa State Aviation Technical University (USATU),
Ufa,
Russia
kudashov.dd@ugatu.su
ORCID 0000-0003-4360-0236

Kseniya Olegovna Novikova
Ufa State Aviation Technical University (USATU),
Ufa,
Russia
novikova.ko@ugatu.su
ORCID 0000-0002-2669-9185